Large Shear Box Tests on Two Geogrid Reinf Orced Soils

F. Moghadas Nejad
Assistant Professor
Civil Engineering,
Amirkabir University of Technology

Abstract

The goal of this research is to measure the interface properties between a geogrid and a soil (i.e. the friction angle and dilatancy angle) as well as the strength parameters of materials used in the tests in order to be able to use the parameters in numerical analysis. A comprehensive set of large shear box tests were conducted on the geogrid. Apart from the main findings, some interesting results concerning the mechanisms behind the behaviour of reinforcement in direct shear tests were obtained.

Keywords

Geogrid, Shear box Test, Reinforced Soi.

Introduction

The tests were carried out using a large shear box. The various components of the apparatus are described and then the results are presented and discussed. However, firstly a background of direct shear tests on soil reinforcement is presented briefly.

Literature Review

Bergado et al. [1] carried out several large scale direct shear box with various normal stresses using Weathered Bangkok clay as wall backfill material and Tensar grid as a reinforcement laid horizontally at the shear plane. Their results showed that the soil/geogrid interface yielded lower peak strength but higher residual strength than that of a soil to soil shear plane due to the resistance from grid apertures to the total residual resistance, especially in the case of low applied normal pressure.

Hausmann and Clarke [2] conducted a series of tests on fly ash with and without reinforcement using a large shear box apparatus including single set-up tests in which a sample was tested in stages under four different normal stresses. The geogrid used was Tensar SS2. They found that the fly ash/geogrid peak shear resistance was significantly lower than the internal shear strength of fly ash alone but that the difference in residual shear resistance was much less. Thus, they suggested that sliding on the ash/geogrid interface should be used to analyse potential failure wedges.

Palmeira and Milligan [3] carried out a comprehensive instrumented large shear box test with geogrid oriented at various angles to the vertical. They concluded that the presence of a reinforcement layer aligned in the direction of the principal tensile strain (which was approximately 30 degrees to the vertical direction) causes a remarkable increase in the shear strength.

Bergado et al. [4] conducted an additional experimental program on a clay using a pullout box and large scale shear devices. For both pull-out and direct shear tests, a multistage procedure was used. Their direct shear test result showed that the friction angle obtained from the shear box for the soil only was substantially lower than the UU-triaxial test result. The reason was that for large scale direct shear tests, the shear surface is progressively formed owing to the compressive deformation of the soil specimen. Consequently the peak shear strengths along the predetermined shear surface are not mobilised at the same time and the measured strength parameters are lower than those of the triaxial UU test. A similar result was also obtained by Potts et al. [5]. Therefore, they recommended that in actual cases such as a slope failure surface, where the failure surface is formed progressively, the large scale direct shear box test result is more suitable for actual design. Furthermore their results on Tensar SS2 indicated that the soil/grid reinforcement interface can provide the same shear strength as the soil itself.

A comprehensive set of unreinforced and reinforced direct shear tests on sand has been conducted by Jewell and Wroth [6]. In these tests a number of close-coiled tension springs were used to model circular, rough, perfectly elastic reinforcement bars and in some tests a steel rod was inserted into each spring and secured at both ends to increase the stiffness of the spring. Direct shear tests were carried out on the reinforcement which was placed at various orientations. In the unreinforced tests, the results showed that the tangent of the angle of friction from direct shear tests is about 20% less than the tangent of the plane strain angle of friction (plan strain test). Thus performing a stability analysis by using a direct shear angle of friction for compacted granular material is conservative with a safety factor of 1.2 for both the peak strength and the critical state strength. In a direct shear test on a reinforced soil, Jewel's results indicated that the reinforcement has almost no influence on shearing resistance until the mobilised shearing resistance in the sand exceeds a certain value and the amount of improvement at any shear displacement depends on the stiffness of the reinforcement and the benefit increases as the soil continues to deform. As well, the vertical displacement in reinforced sand tests compared with the unreinforced test was larger, and this indicates that the reinforcement causes more sand to deform and helps to resist localised shear deformation. Jewell also observed by radiography that reinforcement improves the shearing resistance of the soil by directly reducing the disturbing shear force acting on the soil, and by increasing the available frictional shearing resistance in the soil. Based on their findings, the best position of reinforcement is close to the direction of principal incremental tensile strain in the soil (about 30 degrees to the vertical direction). This confirms the Palmeira and Milligan [3] result which was mentioned earlier. In the case of horizontal reinforcement placed at the shear plane, improvement in shear resistance was found to be zero. Also their analysis and observations for a few tests with reinforcement placed at angles of between 23 to 25 degrees to the vertical, showed that because the ratio of the principal incremental tensile to compressive strain increases with the angle of dilation, considerably less deformation is required to generate reinforcement force in dense sand than in loose sand. Finally they suggested that the maximum angle of friction which could be measured in a modified direct shear test on perfectly rough reinforcement would also be equal to the direct shear angle of friction, ϕ_{ds}, for soil to soil shearing.

As may be seen from the above, the majority of researchers suggest that;

- there is no improvement due to reinforcement in direct shear box tests if reinforcement is placed horizontally and,
- The best orientation for reinforcement to have the optimum influence on shear strength is close to the direction of principal tensile strain.

Large-Scale Direct Shear Box Devices

A schematic diagram of the large direct-shear apparatus is shown in Figures 1a,b. It has a shear area of 0.003 m^2 (0.305m x 0.305m) with a total depth of 0.16 m. The shear force is applied by an electro-hydraulically controlled jack through a steel reaction frame. The shear capacity of this equipment is 5 tons. The outer box (B) sits on two steel channels with roller bearings (A) making it possible to displace the lower half of the shear box in the shear direction. The shear force is applied to the lower half of the box through a steel plate (C) welded to the outer box and bearing on the lower half of the shear box just below the shear plane. In order to measure the shear force, a reaction system is provided consisting of two parallel steel bars (D) connected to the upper half of the box. These two horizontal bars apply the reaction force to a steel proving ring (E). Deformation of the ring is monitored by using a Liner Variable Differential Transducer (L.V.D.T) supplemented by a dial gauge. The radial displacement of the ring is calibrated against load applied to it. The normal stress is applied on the top plate through a horizontal rectangular section beam connected to two vertical bars (F). These bars are again connected to a similar horizontal beam to which a force is applied through a lever beam, (H). At the end of the lever beam there is a hanger for placing the weights. The normal load applied to the shear box is calculated by taking moments about the fulcrum of the lever. The rate of shearing is electrically controlled and a shear rate of 2 mm/min. was adopted. The horizontal and vertical displacement were also monitored by an L.V.D.T supplemented by a dial gauge in order to provide a check of the transducer readings. The voltage output from the transducers is transformed through a data acquisition box to digital values and is recorded by a personal computer. In each test, the same weight of soil was added to the same depth in the box, so that from test to test the void ratio of the sample remained the same. In all tests the soil was compacted in four layers with equal thickness and each layer was compacted by an impact hand compactor and given the same number of blows per layer. A view of the apparatus is shown in Figure 1c.

TEST MATERIALS

Two kinds of soils are selected for testing (Fig. 2).

The first soil is crushed aggregate of basaltic origin and of 5-mm nominal size with particles that are mainly subangular. The D_{10} and D_{60} sizes measured are about 2.0 mm and 4.0 mm respectively, which gives a uniformity coefficient of 2.0. This may be classified as a uniform fine gravel with less than 1% of particles finer than 75 μm.

The second soil is silica sand called Sydney sand. The D_{10} and D_{60} of this material are about 0.25 and 0.37 respectively, which gives a uniformity coefficient of about 1.5. This means that the soil can be classified as well-graded sand with less than 1% of fines.

The geogrid used in this research is Tensar SS2, which is manufactured from polypropylene. Typical dimensions of the geogrid are presented in Fig. 3.

TEST RESULTS

Generally the direct shear resistance developed between a geogrid and a soil is composed of three components;

- Shear resistance between the soil and the plan surface area of the geogrid,
- The soil to soil shear resistance over the geogrid openings,
- The resistance from soil bearing on the geogrid apertures (Jewel et al. 1984).

As will be shown later, the third component is difficult to assess in a shear box test and so it is assumed to be included in the shearing resistance. Therefore, direct shear resistance can be expressed in terms of the two contributions from shear between the soil and the plan surface area of the reinforcement and the shear between soil and soil.

Four comprehensive test series were carried out including direct shear tests on;

I- Subgrade material (sand) alone or a reinforced sand with sand above and below the geogrid.

II- Base material (5mm aggregate) alone or a reinforced 5mm aggregate with 5mm aggregate above and below the geogrid.

III- Sand above and 5mm aggregate below the geogrid (shear plane at the sand-geogrid interface).

IV- 5mm aggregate above and sand below the geogrid (shear plane at the 5mm aggregate-geogrid interface).

Figure 4 shows the shear box configuration for the above tests.

1-Subgrade material (sand) alone and reinforced sand with sand above and below the geogrid (Series A).

Figures 5 a,b show the results of the shear box tests. It is clear from these figures that there is no improvement in shear resistance at peak and critical states due to the geogrid. The angle of dilation and angle of friction at peak resistance and at the critical state for the unreinforced and the reinforced sand are presented in Table 1 for all of the cases A to D. The angle of friction at the peak may be seen to be almost the same for both the reinforced and the unreinforced cases, probably due to the fact that majority part of geogrid surface are openings (about 82%).

At the residual state, the critical state friction angle in the unreinforced sand is slightly higher than that of the reinforced one. This is also suggested in Figure 5b because dilation at the critical state is higher in the unreinforced sand under all normal stresses. The angle of friction at the peak and the critical states were determined by fitting the line of best fit to the results in Figures 6 a,b.

2-Base material (5mm aggregate) alone and reinforced 5mm aggregate with 5mm aggregate above and below the geogrid (Series B).

Figures 7a,b and 8a,b show the results of this series of tests. Shear resistance at both the peak and critical states is higher in the unreinforced base material than that of the reinforced material. The angle of dilation at peak (Table 1) also suggests this difference. Higher dilation at the critical state in unreinforced 5mm aggregate (Figure 7b) indicates more mobilised shear resistance in the unreinforced 5mm aggregate.

3-Sand above and 5mm aggregate below the geogrid (Series C).

In order to determinate the properties of the interface of the subgrade and the geogrid, the shear plane must be forced to occur along the sand-geogrid interface. Thus the base material (5mm aggregate) was placed in the lower half of the box and then the geogrid was placed over the lower half of the box and finally the base material was placed in the upper half of the box and compacted (Figure 4).

Figures 9a,b and Figure 10 show the results of this series of tests. The angle of friction and dilation at peak shear resistance and the angle of friction at the critical state have been presented in Table 1.

4- 5mm aggregate above and sand below the geogrid (Series D).

In these tests (like series C) the purpose of the test was to determinate the properties of the base-geogrid interface. Thus, sand was placed in the lower half of the box in two layers and compacted, then the geogrid was placed at the top of the lower half of the box beneath the shear plane and finally base material (i.e. 5mm aggregate) was placed in two layers in the upper half of the box and compacted.

Results are shown in Figures 11a,b and Figure 12. Table 1 presents the angle of friction and dilation at the peak and the critical angle of friction.

DISCUSSION

In the following, the importance of the components of shear resistance is examined.

If the bearing capacity of the geogrid apertures is not taken into account, the following equation can be used to express the relation between the angle of friction of all parts of the interface.

$\tan \phi_{sg} = \alpha_g \tan \phi_g + (1 - \alpha_g) \tan \phi$ Bergado et al. [1] (A)

where

ϕ_{sg} friction angle between soil and geogrid reinforcement (including openings)

ϕ_g friction angle of soil and geogrid surface

ϕ friction angle of soil

α_g fraction of surface area occupied by geogrid ($\cong 0.2$ for Tensar SS2)

The angle of shearing resistance at the geogrid-soil interface is examined further in The Appendix.

SUMMARY AND CONCLUSIONS

The following conclusions can be drawn from the test results presented in this section:

1-If a geogrid is placed horizontally no improvement is caused in shear resistance (along the geogrid-soil interface) due to the presence of the geogrid.

2-Eq. A is applicable to the direct shear test at the peak resistance.

3-At peak state, shear resistance of a reinforced soil has two components; shear resistance between the soil and geogrid plan surface area, and soil to soil resistance at the geogrid openings. Bearing capacity forces against the cross-members of the geogrid are small in a shear box test at peak state.

4-The components of the shear resistance acting on the shear plane can be estimated quantitatively.

5-No improvement in shear resistance was found due to horizontal reinforcement placement. This confirms the Pamlmira and Milligan [3] as well as Jewell and Worth [6] findings.

6-Due to rotation and tilting of the upper half of the shear box at large displacement, the shear plane may not have occurred at the soil-geogrid interface at critical state.

Table (1) Dilatancy angle and friction angle measured from large shear box tests.

	Ψ_p	ϕ_p	$\phi_{cr(deg.)}$
Sand (subgrade)	7.26	34.69	31.03
Sand + geogrid	8.27	34.52	30.11
5mm aggregate (base)	15.28	45.86	40.12
5mm aggregate + geogrid	14.58	45.58	39.58
Sand + geogrid + 5mm aggregate (shear plane at sand-geogrid interface)	10.64	36.07	31.43
5mm aggregate + geogrid + sand (shear plane at 5mm aggregate-geogrid interface)	9.47	39.07	37.39

APPENDIX

The angle of shearing resistance at the geogrid-soil interface is examined further in this Appendix.

A- At peak resistance.

a- Series A;

From Table 1 we have,

$\phi_{sg} = 34.52^\circ$ From reinforced sand (Figure 4b)

$\phi = 34.69^\circ$ From sand alone (Figure 4a)

$\alpha = 0.2$

Using Eq. A, the peak friction angle between the sand and the geogrid surface is;

$$\phi_g = 33.83^\circ \quad (1)$$

b- Series B;

From Table 1,

$\phi_{sg} = 45.58^\circ$ From reinforced 5mm. aggregate (Figure 4d)

$\phi = 45.86^\circ$ From 5mm aggregate alone (Figure 4c)

$\alpha_g = 0.2$

Using Eq. A, the peak friction angle between the 5mm aggregate and the geogrid surface,

$$\phi_g = 44.43^\circ \quad (2)$$

c- Series C:

Sand + geogrid + 5mm aggregate (shear plane at sand-geogrid interface)

$\phi_{sg} = 36.07^\circ$ (Figure 4e)

From (1) we have

$\phi_g = 33.83^\circ$

$\alpha_g = 0.2$

From Eq. A, the angle of friction between the sand and the 5mm aggregate at the openings,

$$\phi = 36.65^\circ \quad (3)$$

d- Series D:

5mm. aggregate + grid + sand (shear plane at 5mm. aggregate-geogrid interface)

$\phi_{sg} = 39.07^\circ$ (Figure 4f)

From (2) we have,

$\phi_g = 44.43^\circ$

$\alpha_g = 0.2$

From Eq. A, the angle of friction between the sand and the 5mm aggregate at the openings

$$\phi = 37.58^\circ \quad (4)$$

e- A comparison between the peak angle of friction of the sand and the 5mm aggregate at the openings from two approaches;

$(3) \Rightarrow \phi_{1(peak)} = 36.65^\circ$

$(4) \Rightarrow \phi_{2(peak)} = 37.58^\circ$

$$\Delta\%_{(peak)} = \frac{37.58 - 36.65}{37.58} \times 100 = 2.47\%$$

The results of the two approaches are approximately equal. This suggests that ;

-The shearing has occurred exactly at the geogrid-soil interface.

-Eq. A is applicable in direct shear tests

-Bearing capacity of the geogrid transverse ribs has only a small influence at the peak state in direct shear tests.

B- At critical state

a- Series A:

From Table 1;

$\phi_{sg} = 30.11^\circ$ From reinforced sand (Figure 4b)

$\phi = 31.03^\circ$ From sand alone (Figure 4a)

$\alpha_g = 0.2$

Using Eq. A the critical friction angle between the sand and the geogrid surface is,

$$\phi_g = 25.93^\circ \qquad (5)$$

b- Series B:

From Table. 1,

$\phi_{sg} = 39.58^\circ$ From reinforced 5mm aggregate (Figure 4d)

$\phi = 40.12^\circ$ From 5mm aggregate alone (Figure 4c)

$\alpha_g = 0.2$

Using Eq. A, the critical state friction angle between the 5mm aggregate and the geogrid surface is,

$$\phi_g = 37.36^\circ \qquad (6)$$

c- Series C:

Sand + geogrid + 5mm aggregate (shear plane at sand-geogrid interface)

From Table 1,

$\phi_{sg} = 31.43^\circ$ (Figure 4e)

From (5) we have

$\phi_g = 25.93^\circ$

$\alpha = 0.2$

Using Eq.A the critical state angle of friction between the sand and the 5mm aggregate at the openings is,

$$\phi = 32.71^\circ \qquad (7)$$

d- Series D:

5mm aggregate + grid + sand (shear plane at 5mm aggregate-geogrid interface)

From Table. 1,

$\phi_{sg} = 37.3^\circ$ (Figure 4f)

From (6),

$\phi_g = 37.36^\circ$

$\alpha = 0.2$

Using Eq. A the critical state angle of friction between the sand and the 5mm aggregate at the openings is,

$$\phi = 37.40^\circ \qquad (8)$$

Comparison between the critical state angle of friction between the sand and the 5mm aggregate at the openings from two approaches,

(7)$\Rightarrow \phi_{1(critical)} = 32.71^\circ$

(8)$\Rightarrow \phi_{2(critical)} = 37.40^\circ$

$$\Delta\%_{(critical} = \frac{37.40 - 32.71}{37.40} \times 100 = 12.5\%$$

The result indicates that the difference is higher than for the peak ($\Delta\%$ = 2.47) which shows the shear plan has probably not occurred at the soil-geogrid interface. This may have been due to rotation and titlting the upper half of shear box which was observed at the end of the tests.

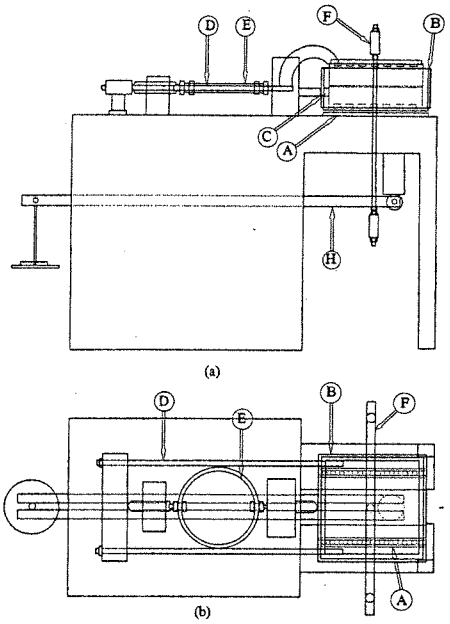

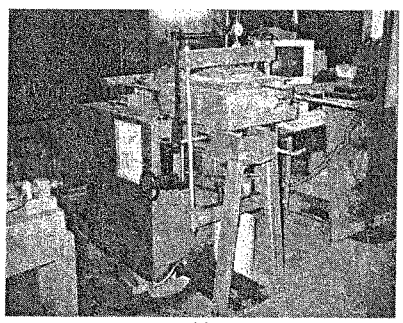

(c)

Figure (1) Large Shear Box
(a) Longitudinal Section, (b) Plan, (c) View

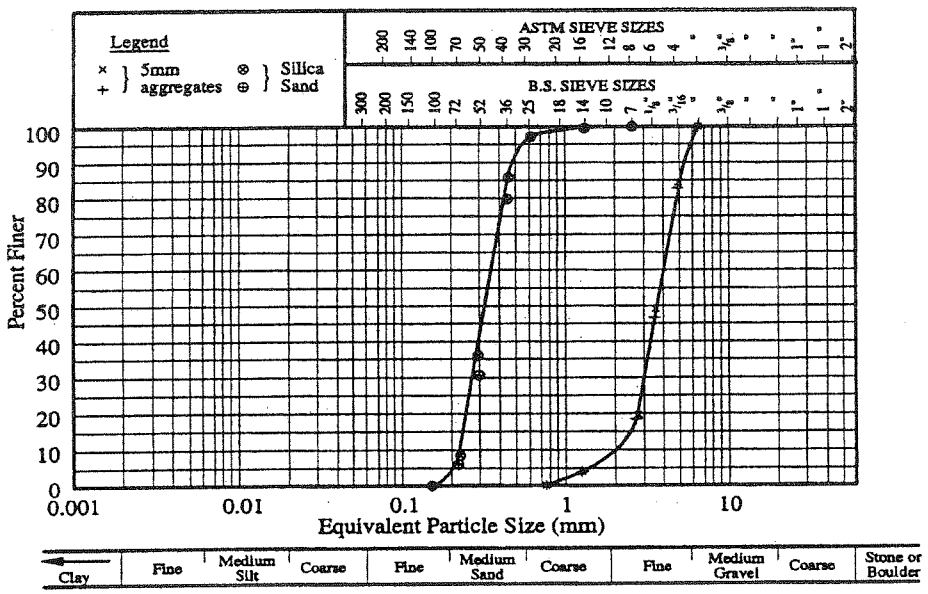

FIGURE (2) PARTICLE SIZE DISTRIBUTION.

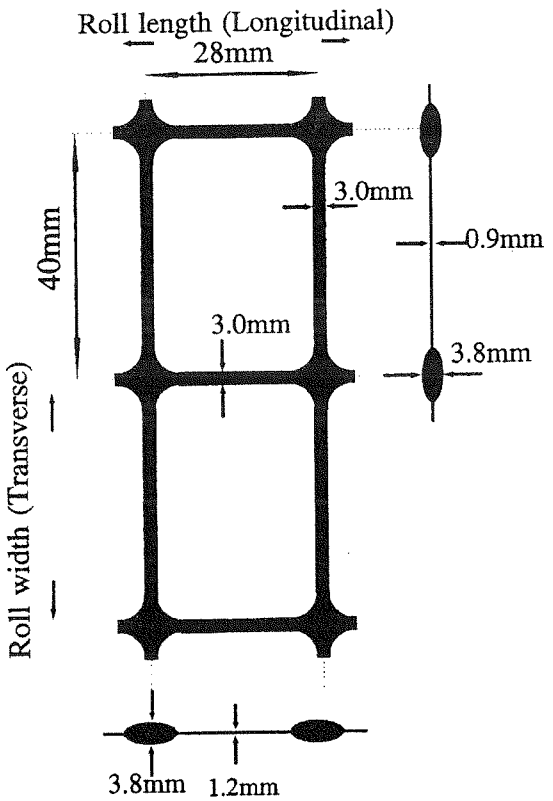

FIGURE (3) GENERAL DIMENSIONS OF TENSAR SS2.

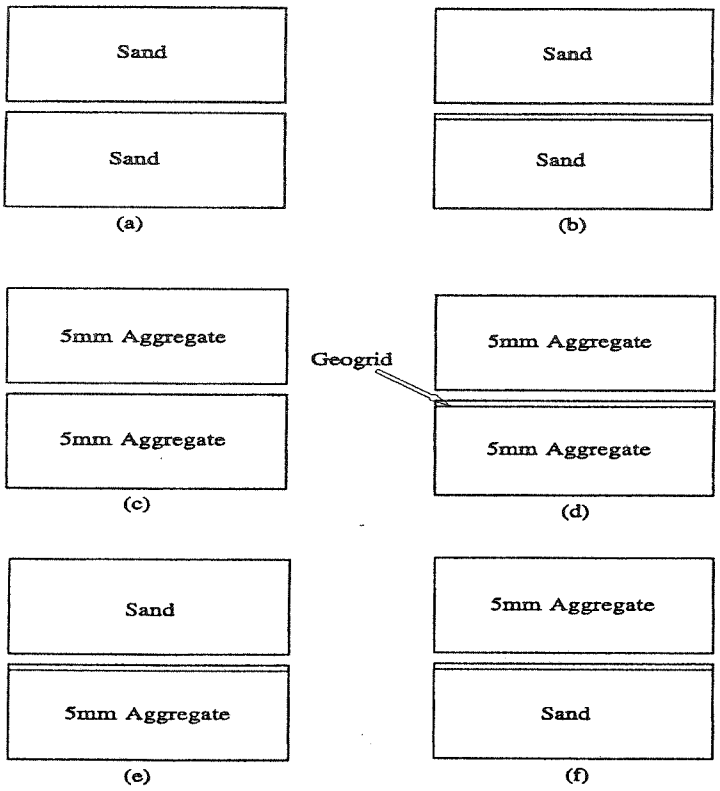

Figure (4) Series of Tests Conducted Using the Large Shear Box.

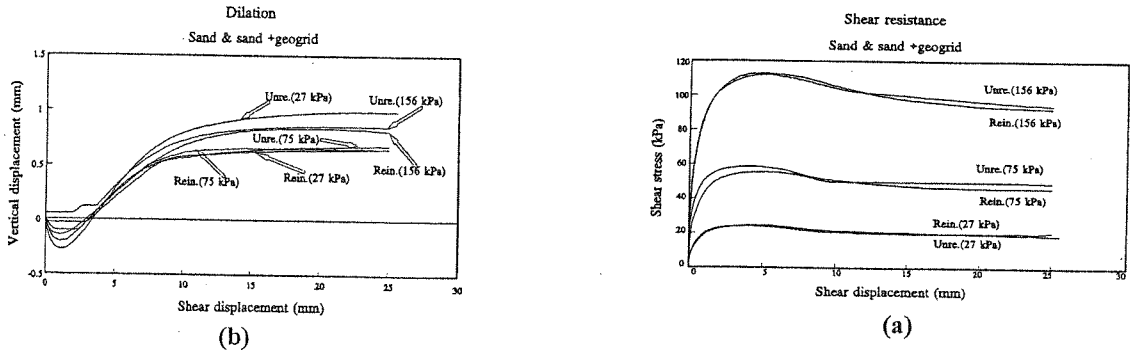

Figure (5) Sand alone and sand plus geogrid.

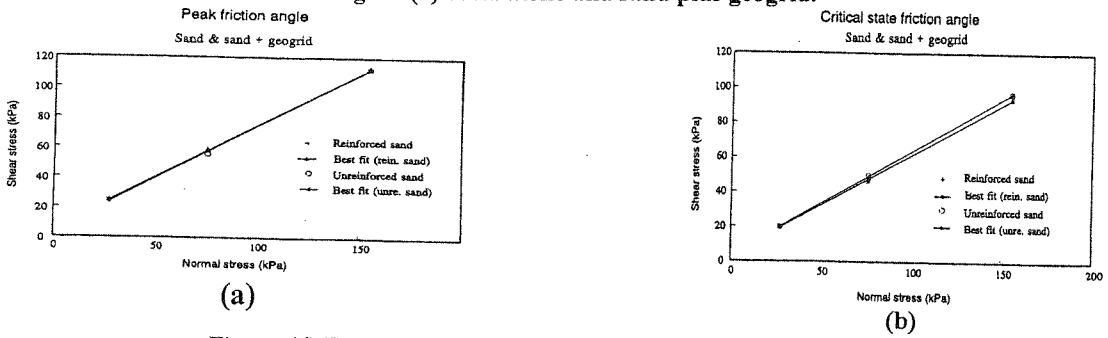

Figure (6) Failure envelopes for sand alone and sand plus geogrid.

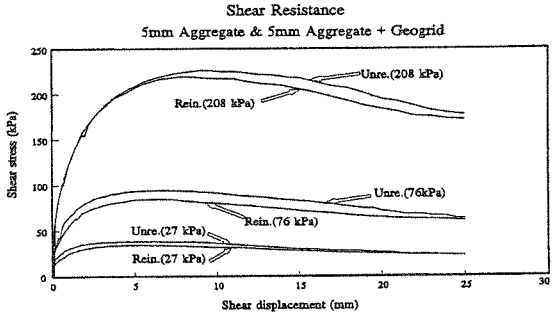

(a)

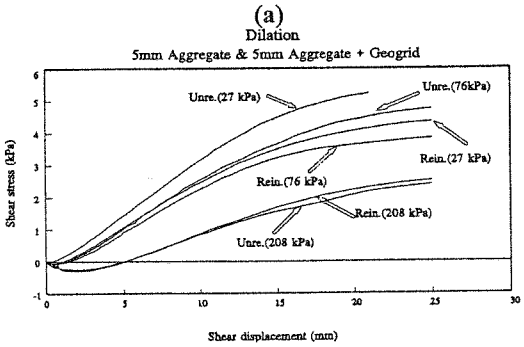

(b)

Figure (7) 5mm aggregate alone and 5mm aggregate plus geogrid.

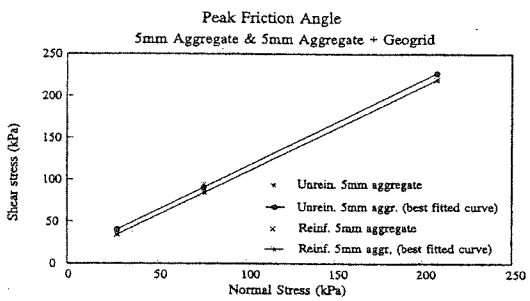

(a)

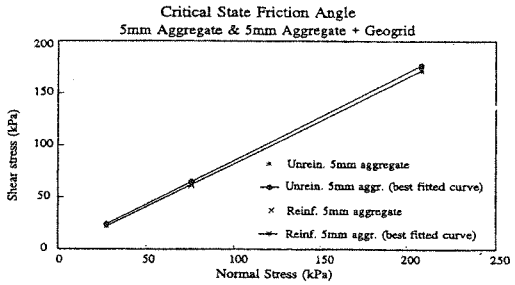

(b)

Figure (8) Failure envelopes for 5mm aggregate alone and 5mm aggregate plus geogrid.

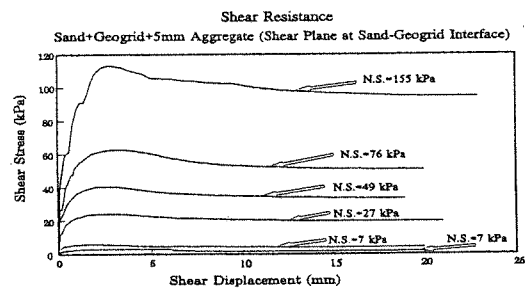

(a)

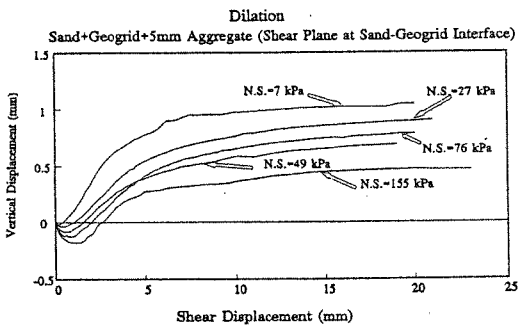

(b)

Figure (9) Shearing at the sand-geogrid interface (sand above 5mm aggregate below the geogrid).

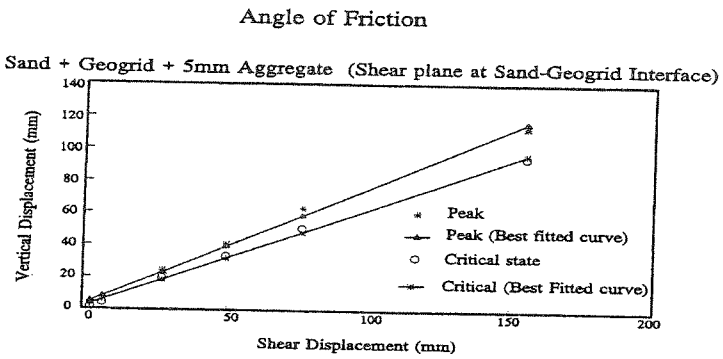

Figure (10) Failure envelope for shearing at sand-geogrid interface (sand above 5mm aggregate below the geogrid).

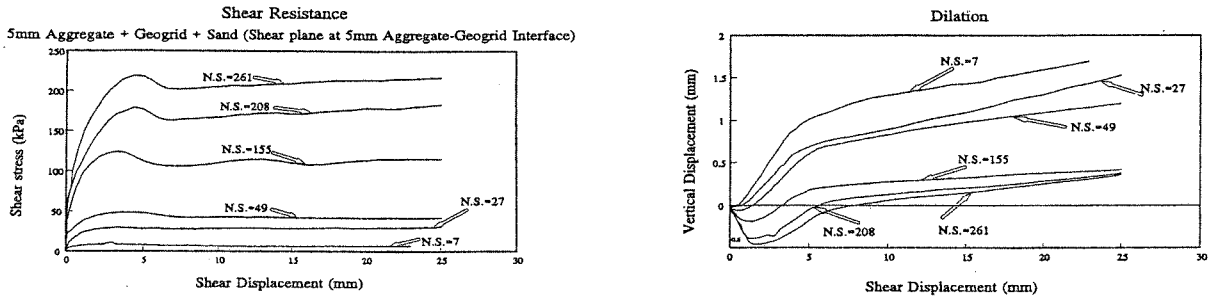

Figure (11) Shearing at the 5mm aggregate -geogrid interface (5mm aggregate above sand below the geogrid).

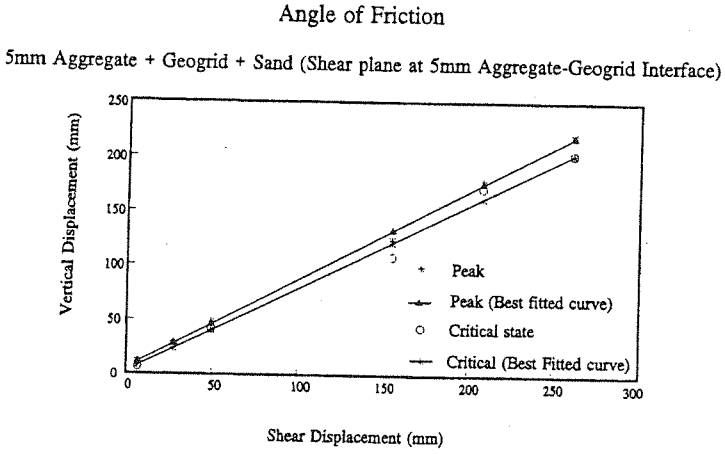

Figure (12) Failure envelope for shearing at the 5mm aggregate -geogrid interface (5mm aggregate above sand below the geogrid).

References

[1] Bergado, D.T., Chai, J.C. and Balasubramaniam, A.S. (1992) "Interaction Between Grid Reinforcement and Cohesive-Frictional Soil", Earth Reinforcement Practice, Balkema, Rotterdam, pp. 29-34.

[2] Hausmann, M.R. and Clarke, J.W. (1994) "Fly Ash/Geogrid Direct Shear Tests", Australian Geomechanics, April 1994, pp. 67-72.